Applied Clay Science 161 (2018) 169–175

Contents lists available at ScienceDirect

Applied Clay Science

journal homepage: www.elsevier.com/locate/clay

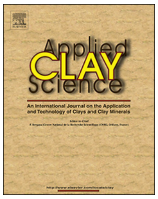

Research paper

The preferential retention of $^{\mathrm{VI}}$Zn over $^{\mathrm{IV}}$Zn on birnessite during dissolution/desorption

Zhangjie Qin[a,b], Hui Yin[a], Xiaoming Wang[a], Qin Zhang[b], Shuai Lan[a], Luuk K. Koopal[c], Lirong Zheng[d], Xionghan Feng[a], Fan Liu[a,*]

[a] *Key Laboratory of Arable Land Conservation (Middle and Lower Reaches of Yangtze River), Ministry of Agriculture, College of Resources and Environment, Huazhong Agricultural University, Wuhan 430070, China*

[b] *Key Laboratory of Poyang Lake Basin Agricultural Resource and Ecology of Jiangxi Province, College of Land Resource and Environment, Jiangxi Agricultural University, Nanchang 330045, China*

[c] *Physical Chemistry and Soft Matter, Wageningen University, Dreijenplein 6, 6703 HB Wageningen, The Netherlands*

[d] *Beijing Synchrotron Radiation Facility, Institute of High Energy Physics, Chinese Academy of Sciences, Beijing 100039, China*

ARTICLE INFO

Keywords:
Zinc coordination
Birnessite
Dissolution
Desorption
Extended X-ray absorption fine structure spectroscopy

ABSTRACT

Zn is a common heavy metal in soils and sediments. In this study, the release behaviors of octahedral ($^{\mathrm{VI}}$Zn) and tetrahedral ($^{\mathrm{IV}}$Zn) Zn complexes on synthesized hexagonal birnessite were explored by solution chemistry method in combination with spectroscopic analysis. In acidic dissolution processes, the release of adsorbed Zn^{2+} from birnessite occurred into two stages: in the first stage, ~60% of Zn^{2+} was desorbed rapidly, with only 8% of Mn being released, and the ratio of $^{\mathrm{VI}}$Zn/$^{\mathrm{IV}}$Zn increased with time; in the second stage, the residual Zn^{2+} was mostly $^{\mathrm{VI}}$Zn and released slowly at a nearly constant rate until complete dissolution of the matrix mineral was observed. During desorption of Zn^{2+} by Pb^{2+}, the ratio of $^{\mathrm{VI}}$Zn/$^{\mathrm{IV}}$Zn on birnessite also increased, while the residual percentage of $^{\mathrm{VI}}$Zn remained nearly constant. However, it is known that $^{\mathrm{IV}}$Zn-triple corner-sharing (TCS) is more stable than $^{\mathrm{VI}}$Zn-TCS, suggesting that part of the remaining $^{\mathrm{IV}}$Zn-TCS on birnessite might transform to $^{\mathrm{VI}}$Zn-TCS immediately when $^{\mathrm{VI}}$Zn-TCS is replaced by H^+ or Pb^{2+}. Additionally, the possible distribution of Mn^{3+} and $^{\mathrm{IV}}$Zn or the partial charge compensation by protons can lead to the preferential retention of $^{\mathrm{VI}}$Zn on birnessite or the preferential re-adsorption of $^{\mathrm{VI}}$Zn at the new edge sites. These results can provide new insights into the geochemical behavior of Zn^{2+} contaminant in soil and aquatic environments.

1. Introduction

Zinc is an important transition metal, and an essential element for all living organisms. However, mining, smelting and industrial activities have led to high Zn^{2+} concentrations in regional areas, which poses a great threat to those environments (Chaney, 1993; Roberts et al., 2003). Manganese (Mn) oxides as one kind of important adsorbents in environment, have significant impacts on the geochemical cycles of metal ions in soils, aquifers, and sediments, especially Zn^{2+} (Fuller and Harvey, 2000; Manceau et al., 2003; Olivie-Lauquet et al., 2001; Saunders et al., 1997).

There are > 30 kinds of Mn oxides in nature, among which the nanosized and layered birnessite is ubiquitous and known for its high reactivity toward adsorption and redox reactions in soils, sediments, and seafloors (Frierdich et al., 2011; Liu et al., 2002; Post, 1999; Villalobos et al., 2003, 2006; Vodyanitskii, 2009). It consists of stacked layers of edge-sharing MnO_6 octahedra with a layer-to-layer distance of ~7.2 Å (Drits et al., 1997; Giovanoli, 1969). Substitutions of the layer Mn^{4+} by other lower-valence cations (such as Mn^{3+} and Co^{3+}) and octahedral vacancies lead to deficits of positive charges (Lanson et al., 2000, 2002; Silvester et al., 1997; Villalobos et al., 2006; Webb, 2005; Yin et al., 2011). Birnessite tends to adsorb alkali and alkaline-Earth cations (e.g., Na^+, K^+, Ca^{2+}, Pb^{2+}, Cu^{2+}, Zn^{2+}, Mn^{2+}, Mn^{3+}, Cd^{2+}, and Ni^{2+} etc.) in the interlayer regions and/or at the vacancies and edge sites (Drits et al., 1998, 2002, 2007; Lanson et al., 2008; Manceau et al., 2002a; Peña et al., 2010; Peacock and Sherman, 2007; Webb, 2005). The sorption affinity of birnessite for metal cations decreases in the order $Pb^{2+} > Cu^{2+} > Zn^{2+} > Ni^{2+} > Cd^{2+} > Ca^{2+}$ (Benjamin and Leckie, 1981; Kinniburgh et al., 1976; van Genuchten and Peña, 2016; Wang and Stumm, 1987).

These heavy metals (e.g., Ni^{2+}, Cu^{2+}, Zn^{2+}, and Pb^{2+}), when adsorbed onto birnessite surface vacancies, mainly from triple-corner-sharing (TCS) inner-sphere complexes with octahedral and/or tetrahedral geometry, as demonstrated by powder X-ray diffraction (XRD)

---

[*] Corresponding author.
E-mail address: liufan@mail.hzau.edu.cn (F. Liu).

https://doi.org/10.1016/j.clay.2018.04.017
Received 5 January 2018; Received in revised form 5 April 2018; Accepted 13 April 2018

and extended X-ray absorption fine structure (EXAFS) analyses (Lanson et al., 2002; Manceau et al., 2002a; Peña et al., 2010; Peacock and Sherman, 2007; Sherman and Peacock, 2010). Pb^{2+}, Ni^{2+}, Cu^{2+}, and even Zn^{2+}, can be reactive with edge sites to form other adsorption structures such as triple-edge-sharing (TES), double-corner-sharing, and double-edge-sharing structures, depending on the reaction conditions (Drits et al., 2002; Kwon et al., 2010; Lanson et al., 2002; Manceau et al., 2002a; Peña et al., 2015; Simanova et al., 2015; Takahashi et al., 2007; Villalobos et al., 2005). Metal ions such as Ni^{2+} and possible Cu^{2+}, can also incorporate (INC) into the vacancies depending on the environmental conditions (Manceau et al., 2007a; Sherman and Peacock, 2010).

Among these heavy metals, Zn^{2+} is very interesting for the formation of octahedral and tetrahedral complexes on birnessite vacancies (Kwon et al., 2009, 2013; Manceau et al., 2002a; Toner et al., 2006). It has been reported that Zn^{2+} adsorbs onto δ-MnO_2 at pH 5.5 only in the form of ^{VI}Zn (Li et al., 2004). Manceau et al. (2002a) and Lanson et al. (2002) found that at pH 4 and a low adsorption loading, Zn^{2+} was adsorbed as ^{IV}Zn-TCS located at the birnessite vacancies, while at high adsorption loading, ^{VI}Zn was the predominant adsorption species (Lanson et al., 2002; Manceau et al., 2002a). Additionally, Grangeon et al. (2012) found that at pH 5 and pH 7, Zn^{2+} was predominantly adsorbed as ^{VI}Zn-TCS complexes at high adsorption loading. Regarding the stability of ^{VI}Zn-TCS and ^{IV}Zn-TCS, Manceau et al. (2002a, 2007b) hypothesized that ^{IV}Zn-TCS complexes on birnessite favorably occur to compensate charge deficits of vacancy sites, which is more effective than ^{VI}Zn-TCS at a low Zn/Mn ratio. Kwon et al. (2009) proposed that ^{IV}Zn-TCS shows slightly higher stability than ^{VI}Zn-TCS on birnessite without the need for Mn(III) substitution using density functional theory (DFT) calculations of the total electronic energies of the two isolated isomers, further confirming the hypothesis proposed by Manceau et al. (2002a, 2007b). Furthermore, Kwon et al. (2009) proposed a possible transformation between ^{IV}Zn-TCS and ^{VI}Zn-TCS depending on external conditions, which remain undefined. In addition, the magnetic moments of unsaturated surface O (Mn_2—O) with cations at the vacancy sites are $-0.04\ \mu_B$ for Mn_2—O—H, $+0.04\ \mu_B$ for Mn_2—O—^{IV}Zn—TCS and $+0.08\ \mu_B$ for Mn_2—O—^{VI}Zn-TCS (Kwon et al., 2009), indicating that the protonation of unsaturated surface O could affect the proportions of ^{IV}Zn-TCS and ^{VI}Zn-TCS to balance the magnetic moments of the unsaturated surface O.

To further investigate this, laboratory desorption experiments of Zn on the birnessite vacancies were performed in HCl or Pb^{2+} solutions at different concentrations. Zn K-edge X-ray adsorption near-edge structure (XANES) spectroscopy analysis of the selected samples during the reaction was carried out using a linear combination fitting method to investigate the transformation between ^{VI}Zn and ^{IV}Zn on birnessite. These results revealed the detailed changes between different coordination geometries of adsorbed Zn^{2+} on birnessite during the desorption, which further expounds on the release and migration mechanism of Zn contaminant in the environment.

2. Materials and methods

2.1. Sample preparation

Hexagonal birnessite was prepared according to the procedure reported by McKenzie (1971) via the reduction of boiling $KMnO_4$ solution in the presence of HCl solution. The suspension was cooled and aged at 60 °C for 12 h. The obtained sample was washed with ultrapure water, dried at 40 °C for several days, then ground, and sieved (100 mesh). The final product was stored in a tightly-closed container at room temperature and referred to as HB.

The experiment on the adsorption of Zn to birnessite was conducted in a constant electrolyte solution ($NaNO_3$, 0.1 M). $Zn(NO_3)_2$ solution (137 mL, 0.01 M, pH 4) was added to a 200 mL HB suspension (4 g/L) at pH 4 aiming at a Zn/Mn molar ratio of ~0.138. The mixture was reacted at 25 °C for 24 h with stirring. During the reaction, the suspension pH was maintained at 4 ± 0.05 by adding 0.1 M HNO_3 or 0.1 M NaOH solution, using a pH-stat technique. The sample was filtered, rinsed with the same constant electrolyte solution, and dried at 40 °C for several days. The sample was then ground, stored in a tightly-closed container at room temperature, and called Zn138.

2.2. Characterization

HB and Zn138 were characterized by powder XRD measurements performed on a Bruker D8 Advance diffractometer equipped with a LynxEye detector using Ni-filtered Cu *Kα* radiation ($\lambda = 0.15418$ nm) at a tube voltage of 40 kV and a tube current of 40 mA with 1.2 s of counting time per 0.02° 2θ step. Sample chemical compositions were determined as follows: a 0.1000 g sample was dissolved in 25 mL $NH_2OH{\cdot}HCl$ (0.25 M) and H_2SO_4 (1 M). The metal ion content was measured by atomic absorption spectroscopy (AAS, Varian AAS 240FS) and flame spectrometry (Sherwood Model 410). The average oxidation state (AOS) of manganese was analyzed using the Combo method, in which the 1st derivatives of Mn K-edge XANES spectra of the samples were reconstructed by a weighted sum of all 17 reference spectra in the database with the fractions of species constrained to be non-negative (Manceau et al., 2012). Crystallite morphologies of the samples were probed by field emission-scanning electron microscopy (FE-SEM; JSM-6700F).

2.3. Desorption behavior of Zn from birnessite by H^+ or Pb^{2+}

Acidic dissolution experiments were conducted as described by Yin et al. (2014). Briefly, 0.2000 g of HB or Zn138 sample was slowly dissolved at 35 °C in 500 mL of a 2 M HCl solution. During the dissolution process, the suspension was continuously stirred, and sample aliquots (5 mL each) were withdrawn at predetermined intervals and filtered immediately through a 0.22 μm membrane filter. The concentrations of Mn^{2+} and Zn^{2+} in the filtrates were analyzed using a Varian AA240FS atomic absorption spectrometer. The metal (Me = Mn or Zn) dissolution proportion, X_{Me}, was calculated as $X_{Me} = Me(t)/Me(total)$, where *Me(t)* is the dissolved Me (mol) at time *t*, and *Me(total)* is the total *Me* content (mol) in the sample.

The desorption isotherm of Zn138 was conducted in the presence of 10 or 20 mL of Pb^{2+} solution (0.01 M $Pb(NO_3)_2$ + 0.1 M $NaNO_3$) in 300 mL of a mineral concentration of 0.67 g/L with 0.1 M $NaNO_3$ as the background electrolyte. The suspension was constantly maintained at pH 4.00 ± 0.05 using a pH-stat technique during the reaction. The suspensions were shaken at 200 r/min and 25 °C for 24 h. Pb^{2+} and Zn^{2+} in the solutions were analyzed by AAS. The samples prepared in the presence of 10 and 20 mL of Pb^{2+} solution were named Zn138-Pb0.1 and Zn138-Pb0.2, respectively. In addition, the added Pb ions did not precipitate as $Pb(OH)_2$ since the solubility product constant of Zn138-Pb0.2 (6.7×10^{-24}) was smaller than that of $Pb(OH)_2$ (1.42×10^{-20}) at 289 K.

2.4. Extended X-ray absorption fine structure (EXAFS) spectroscopy

The XAFS spectra were collected using fresh and wet samples rinsed with deionized water at room temperature at the 1W1B beamline of the Beijing Synchrotron Radiation Facility (BSRF) (Yin et al., 2012, 2013). Fluorescence-yield Zn *K*-edge EXAFS spectra were obtained over the range 9459–10,459 eV, where using a 100% Ar-filled Lytle ion-chamber detector with Cu X-ray filters and Soller slits. The monochromator energy was calibrated using a Zn foil ($E_0 = 9659$ eV) before the samples were run. The average Zn *K*-edge EXAFS spectra were background-subtracted using IFEFFIT/Athena software (Ravel and Newville, 2005), with the following parameters: $E_0 = 9659$ eV, $RbKg = 1.0$ Å, and *k*-weight = 3. The k^3-weighted data were analyzed over the *k*-range of 2.6–10 Å^{-1}.